Earthquakes and Structures, *Vol. 8, No. 4 (2015) 843-857*
DOI: http://dx.doi.org/10.12989/eas.2015.8.4.843

System identification of high-rise buildings using shear-bending model and ARX model: Experimental investigation

Kohei Fujita*, Ayumi Ikeda[a], Minami Shirono[a] and Izuru Takewaki[b]

Department of Architecture and Architectural Engineering, Kyoto University, Kyotodaigaku-Katsura, Nishikyo-ku, Kyoto 615-8540, Japan

(Received April 1, 2014, Revised June 25, 2014, Accepted July 16, 2014)

Abstract. System identification is regarded as the most basic technique for structural health monitoring to evaluate structural integrity. Although many system identification techniques extracting mode information (e.g., mode frequency and mode shape) have been proposed so far, it is also desired to identify physical parameters (e.g., stiffness and damping). As for high-rise buildings subjected to long-period ground motions, system identification for evaluating only the shear stiffness based on a shear model does not seem to be an appropriate solution to the system identification problem due to the influence of overall bending response.

In this paper, a system identification algorithm using a shear-bending model developed in the previous paper is revised to identify both shear and bending stiffnesses. In this algorithm, an ARX (Auto-Regressive eXogenous) model corresponding to the transfer function for interstory accelerations is applied for identifying physical parameters. For the experimental verification of the proposed system identification framework, vibration tests for a 3-story steel mini-structure are conducted. The test structure is specifically designed to measure horizontal accelerations including both shear and bending responses. In order to obtain reliable results, system identification theories for two different inputs are investigated; (a) base input motion by a modal shaker, (b) unknown forced input on the top floor.

Keywords: system identification; high-rise building; shear-bending model; ARX model; experiment

1. Introduction

System identification (SI) techniques play an important role in investigating and reducing gaps between the constructed structural systems and their structural design models and in structural health monitoring for damage detection. In the field of SI, there are many achievements (see, for example, World Conferences on Structural Control; Housner *et al*. 1994, Kobori *et al*. 1998, Casciati 2002, Johnson and Smyth 2006, Fujino *et al*. 2010).

It is well recognized that the modal-parameter SI and physical-parameter SI are two major branches in SI (Hart and Yao 1977, Kozin and Natke 1986). The former is suitable for identifying the overall mechanical properties of a structural system and exhibits stable characteristics

*Corresponding author, Assistant Professor, E-mail: fm.fujita@archi.kyoto-u.ac.jp
[a]Graduate Student
[b]Professor

http://www.techno-press.org/?journal=eas&subpage=7 ISSN: 2092-7614 (Print), 2092-7622 (Online)

in its implementation. This characteristic may be related to the fact that the modal parameters are system performances representing global properties of a structural system. While the latter is important from different viewpoints, e.g., enhancement of reliability and robustness in active controlled structures (Doebling *et al*. 1996, Housner *et al*. 1997, Bernal and Beck 2004) or base-isolated structures, its development is limited due to the requirement of multiple and accurate measurements or the necessity of complicated manipulation. A few approaches have been developed so far in the physical-parameter SI, i.e., the multiple-input-single-output (MISO) approaches pioneered by Bendat and co-workers. These approaches, capable of identifying mechanical properties of structural systems have been generalized to handle a wide range of nonlinear time-variant systems excited by non-stationary signals of arbitrary evolutionary power spectrum form (e.g., Bendat *et al*. 1992, Bendat 1998, Spanos and Lu 1995, Kougioumtzoglou and Spanos 2013). On the other hand, a mixed approach is often used in which physical parameters are identified from the modal parameters obtained by the modal-parameter SI. However, in view of inverse problem formulation, a sufficient number of modal parameters must be obtained for the unique and accurate identification of the physical parameters. This requirement is usually hard to be satisfied.

In this paper, a shear-bending model is used for reliable identification of high-rise buildings. While a shear building model has been a well-used model for system identification (for example Zhang and Johnson 2013), Kuwabara *et al*. (2013) and Minami *et al*. (2013a) introduced a shear-bending model and developed system identification theories for high-rise buildings. However their researches are limited mainly to theoretical ones. The corresponding experimental one is developed here. The proposed method has the following merits: (i) the simplicity of system identification requiring only two consecutive floor data in the identification of the story stiffness for a shear model and a shear-bending model and (ii) the robustness to noise by taking advantage of the ARX model.

2. System Identification algorithm for shear and bending stiffnesses

Fundamental algorithms of system identification for shear and bending stiffnesses of a shear-bending model have been proposed in the references (Kuwabara *et al*. 2013, Minami *et al*. 2013a, b). In this section, the proposed system identification algorithms using floor acceleration records for base input and unknown vibration source are briefly explained. It should be remarked that, since the shear-bending model is an ideal mechanical model, actual buildings and test structures cannot be modeled by this model exactly. In other words, the shear and bending stiffnesses of the shear-bending model depend on the loading distributions.

2.1 System Identification algorithm under base input

Consider a building frame as shown in Fig. 1(a) and an N-story shear-bending model as shown in Fig. 1(b). Comparing with the scheme of the system identification for shear model (Takewaki and Nakamura 2000, 2005, Takewaki *et al*. 2011), the transfer function with respect to absolute horizontal accelerations (also displacements), i.e., the jth-floor acceleration to the (j-1)th-floor acceleration) can be introduced as

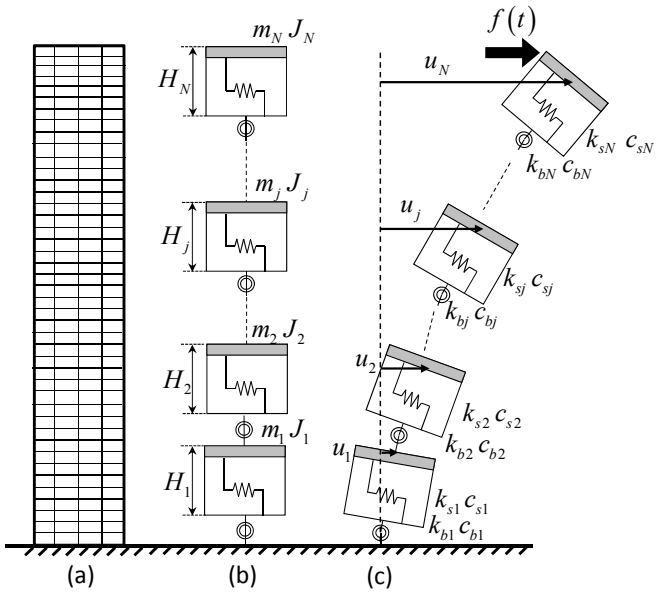

Fig. 1 Shear-bending model

$$G_j = \frac{\ddot{U}_g + \ddot{U}_j}{\ddot{U}_g + \ddot{U}_{j-1}} \tag{1}$$

where $\ddot{U}_g, \ddot{U}_j$ are the Fourier transforms of base and jth-floor accelerations $\ddot{u}_g, \ddot{u}_j$. For evaluating shear and bending stiffnesses, the identification function (*IDF*) is defined in terms of G_j as

$$F_j(\omega) = -\frac{G_{j-1} - 1}{\omega^2 \sum_{i=j}^{N} m_i} \tag{2}$$

By defining the stiffness ratio $R_j \equiv k_{bj}/k_{sj}$ of the bending to the shear, the shear and bending stiffnesses can be formulated as

$$k_{\mathrm{b}j} = \frac{R_j + \dfrac{H_j}{\sum_{i=j}^{N} m_i} \sum_{i=j}^{N} \left\{ m_i (H_i^t - H_{j-1}^t) \right\}}{\lim\limits_{\omega \to 0} \left[\mathrm{Re}\left\{ F_j(\omega) \right\} \right] - \dfrac{H_j}{\sum_{i=j}^{N} m_i} \sum\limits_{m=1}^{j-1} \left[\dfrac{\sum_{i=m}^{N} \left\{ m_i (H_i^t - H_{m-1}^t) \right\}}{k_{\mathrm{b}m}} \right]} \tag{3a}$$

$$k_{\mathrm{s}j} = k_{\mathrm{b}j} / R_j \tag{3b}$$

Assuming that the damping coefficient is in proportion to the stiffness, the relationship between G_j and $G_{j\text{-}1}$ can be derived by considering the dynamic equilibrium of a free body of the shear-bending model as follows

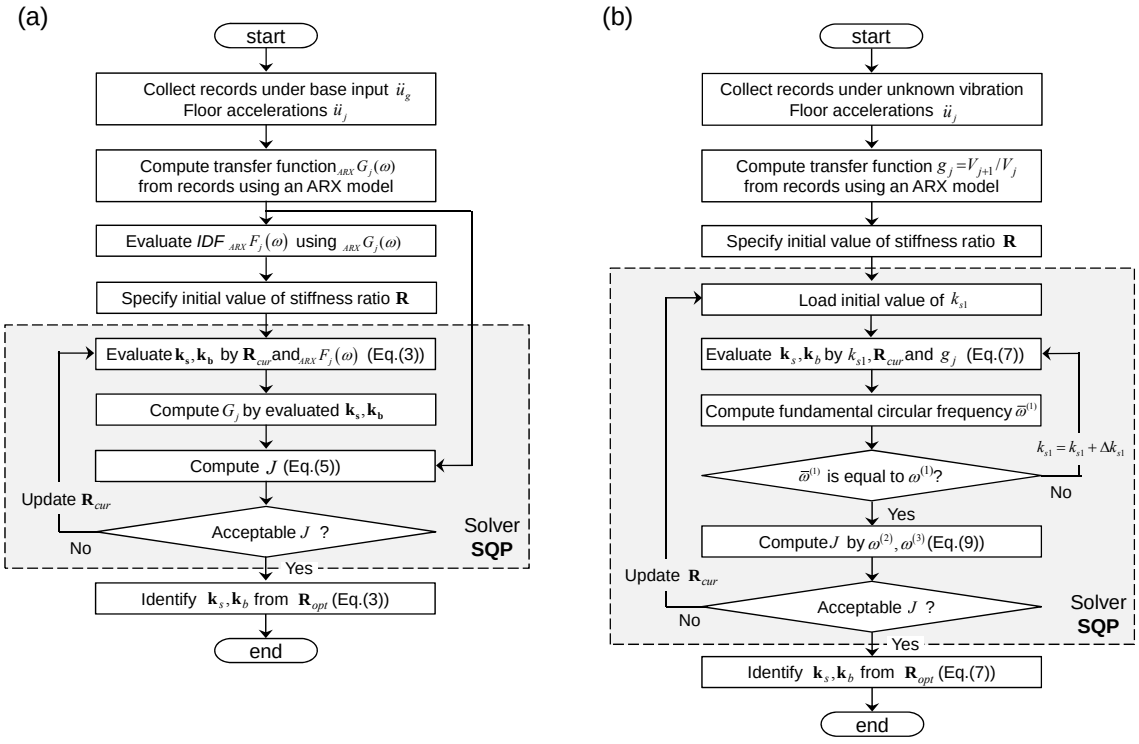

Fig. 2 Flowcharts of two system identification methods; (a) Base input, (b) Unknown internal forced input

$$G_{j-1} = 1/\left[1 + \frac{H_{j-1}\left(1-G_j\right)}{H_j} \left\{ 1 + \frac{\omega^2}{k_{sj} + \mathrm{i}\omega c_{sj}} \sum_{i=j}^{N} \frac{m_i GG(i)}{GG(j-1) - GG(j)} + \frac{\omega^2}{k_{bj} + \mathrm{i}\omega c_{bj}} H_j \sum_{l=j}^{N} \frac{m_l GG(l) \sum_{k=j}^{l} H_k}{GG(j-1) - GG(j)} - \frac{H_j}{H_{j-1}} \frac{\omega^2}{k_{sj-1} + \mathrm{i}\omega c_{sj-1}} \sum_{i=j-1}^{N} \frac{m_i GG(i)}{GG(j-1) - GG(j)} \right\} \right] \tag{4}$$

where H_j, k_{sj}, k_{bj}, c_{sj}, c_{bj} are the structural parameters of the shear-bending model shown in Fig. 1. In addition, $GG(j) = \prod_{k=1}^{j} G_k$. From Eq. (4), it can be observed that the transfer function G_{j-1} is formulated in terms of the transfer functions from the jth through the Nth-story.

Fig. 2(a) shows the flowchart of the proposed system identification method using the floor accelerations under base input. Regarding the stiffness ratios **R** as variable parameters, the stiffnesses are identified so that the transfer function evaluated by Eq. (4) as the function of **R** approximately coincides with that computed by using an ARX model. The SQP (Sequential Quadratic Programming) is applied to find the optimal stiffness ratio **R** so as to minimize the objective function J defined by

$$J=\sum_{j=1}^{N-1}\frac{\sum_{\omega}\left|G_j(\omega,R)-{}_{ARX}G_j(\omega)\right|}{\sum_{\omega}\left|{}_{ARX}G_j(\omega)\right|} \tag{5}$$

2.2 System Identification algorithm under unknown vibration source in structure

Consider the same building model excited by an unknown vibration source $f(t)$ at the top floor as shown in Fig. 1(c). Let V_j denote the Fourier transform of the interstory drift $v_j(=u_j-u_{j-1})$. The transfer function g_j of the interstory drift ratio can be evaluated from the records of floor accelerations as

$$g_j(\omega)\equiv\frac{V_{j+1}(\omega)}{V_j(\omega)}=\frac{U_{j+1}(\omega)-U_j(\omega)}{U_j(\omega)-U_{j-1}(\omega)}\cong\frac{\dot{U}_{j+1}(\omega)-\dot{U}_j(\omega)}{\dot{U}_j(\omega)-\dot{U}_{j-1}(\omega)}\cong\frac{\ddot{U}_{j+1}(\omega)-\ddot{U}_j(\omega)}{\ddot{U}_j(\omega)-\ddot{U}_{j-1}(\omega)} \tag{6}$$

From the estimation of the recurrence relation between the shear stiffness ratio $r_{sj}=k_{sj+1}/k_{sj}$ through the investigation of a few degrees-of-freedom shear-bending model, the shear stiffness ratio r_{sj} can be derived (Minami *et al*. 2013b) as the function of the stiffness ratio R_j and $g_j(\omega)$ as follows

$$r_{sj}=\frac{\left(R_j+H_jH_j^t\right)\prod_{i=1}^{j-1}A_i-H_j\sum_{i=1}^{j}\left(\left(H_i^t\prod_{k=0}^{i-1}A_k\prod_{k=i}^{j}R_k\right)\Big/R_i\right)}{\left(R_{j+1}+H_{j+1}H_{j+1}^t\right)\prod_{i=1}^{j}A_i-H_{j+1}\sum_{i=1}^{j+1}\left(\left(H_i^t\prod_{k=0}^{i-1}A_k\prod_{k=i}^{j+1}R_k\right)\Big/R_i\right)}\left(R_{j+1}+H_{j+1}H_{j+1}^t\right) \tag{7}$$

$$A_i=\begin{cases}1 & (i=0)\\ \left(R_i+H_iH_i^t\right)\lim_{\omega\to0}g_j(\omega) & (i\geq1)\end{cases} \tag{8}$$

where $H_j^t=\sum_{i=j}^{N}H_i$. This recurrence relationship was also proved by the mathematical induction in the reference (Minami *et al*. 2013b). From Eq. (7), by regarding the stiffness ratio $R_i(i=1,2,\ldots,N)$ as the variables, it can be observed that the shear and bending stiffnesses of all the stories can be derived recurrently by specifying the first story shear stiffness.

Fig. 2(b) shows the flowchart of the system identification method for an unknown vibration source. Considering any story stiffness as a leading parameter, the stiffness can be identified so that the fundamental natural circular frequency computed by the eigenvalue analysis is equal to that obtained as the reference value from another record (e.g., microtremor measurement). Then, the stiffness ratios **R** can be determined by the SQP method to minimize the objective function J, i.e., the difference of second and third natural circular frequencies. The objective function used in this system identification method is defined by

$$J=\left|\bar{\omega}^{(2)}-\omega^{(2)}\right|/\omega^{(2)}+\left|\bar{\omega}^{(3)}-\omega^{(3)}\right|/\omega^{(3)} \tag{9}$$

where $\bar{\omega}^{(j)}$ and $\omega^{(j)}$ denote the jth natural circular frequency computed by the eigenvalue analysis of the identified model and the reference one.

3. Experimental verification

Since it is difficult to obtain the true value of shear and bending stiffnesses for existing structures, an experimental verification of the proposed system identification methodology was conducted using a scaled structural model. By comparing the shear and bending stiffnesses identified by the proposed methodologies with those evaluated by the static loading test, the reliability of the proposed system identification methodologies is investigated. As stated above, it should be remarked that, because the shear-bending model is an ideal mechanical model, actual test structures cannot be modeled by this model exactly. The shear and bending stiffnesses of the shear-bending model depend on the loading distributions and the identified stiffnesses in various loading conditions do not necessarily coincide in principle. For this reason, the lower and upper bounds of the shear and bending stiffnesses as the reference value are obtained from the static loading test.

3.1 Design of test structure

The test structure was designed so as to have certain amounts of remarkable shear and bending properties. Fig. 3 shows the schematic diagram of the test structure; floor plates, column plates, spacer blocks (SUS304, 2B) and angle bars supporting columns (steel). The vibration of this test structure along with x axis was investigated as shown in Fig. 3. As a preliminary experiment, vibration tests of a 3-story test structure composed of one column plate in each story were conducted. From that preliminary experiment, it was confirmed that the bending deformation was predominant. In order to obtain an appropriate ratio of shear and bending responses, the test structure was re-designed to have two column plates and adjustable spacer blocks. In this paper, the inner distance between two column plates was set to 10 mm. The base of the test structure was made by a relatively thick stainless plate (14 mm) for the static loading test. In the vibration test for the system identification, the test structure was based on the shake table where the modal shaker was used as the source of the excitation.

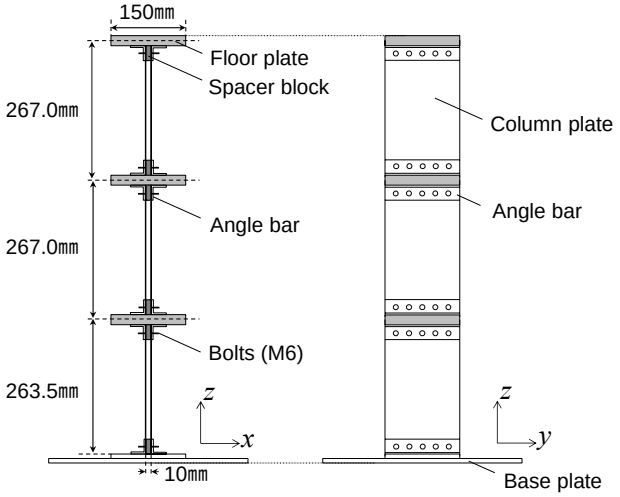

Fig. 3 Schematic diagram of test structure

3.2 Static loading test

For evaluating the reference values of the shear and bending stiffnesses of the test structure for the following system identification, the relationship between force and deformation was investigated by the static loading tests. Figs. 4(a), (b) show the photo of the static loading test; (a) Setup of loading system, (b) Detailed placement of load cell and vertical displacement sensor. For the investigation of the influence of various loading conditions, four different loading variations of the static forces were conducted. The static forces were transmitted through a manually controlled loading system with the load cell (LTS-2KA, *Kyowa Dengyo*). The loading scenarios are summarized in Table 1.

The rotational angle $\theta_i(i=1,2,3)$ of the floor plate was evaluated by measuring vertical displacements of the two points in the same floor mass plate using conventional displacement transducers (CDP-50, *Tokyo Sokki*). As for the horizontal displacement measurement, since the stiffness of the conventional displacement transducer may influence the horizontal stiffness, the horizontal displacement was measured by the laser displacement sensor (IL-300, IL-1050, *KEYENCE*). Fig. 5 illustrates the loading location and displacement sensor positions of the test structure.

The estimated shear and bending stiffnesses k_{si}, k_{bi} $(i=1,2,3)$ from the static loading test were evaluated by the equilibrium equations including measured horizontal displacements and rotational angles of the floor plates which can be evaluated by vertical displacements of the floor plate. These are expressed as

$$k_{si} = \frac{\sum_{l=i}^{3} f_l}{u_i - u_{i-1} - H_i\theta_i}, \quad k_{bi} = \frac{\sum_{l=i}^{3}\left(f_l \sum_{m=i}^{l} H_m\right)}{\theta_i - \theta_{i-1}} \tag{10a, b}$$

where f_i is the static load at the ith floor. Fig. 6 shows the evaluated shear and bending stiffnesses using Eqs. 10(a)-(c) from the static loading test for each scenario. In this static loading test, judging from the measurement system design of the load cell placement, the test structure may be subjected to the bending moment around the center of the floor plate. For this reason undesirable deformation was observed which may be related with instability of the rotation angle of the floor plate. This phenomenon causes a difficulty of the evaluation of shear and bending stiffnesses. For instance, the bending stiffnesses attain large values when the interstory rotation angel $\theta_i-\theta_{i-1}$ is small. This is because, even though the static loading at the top story floor keeps increasing, the interstory rotation angle $\theta_i-\theta_{i-1}$ varies from the negative value in the low-level deformation to the positive value in the high-level deformation.

Table 1 Loading scenario of static forces

		First story	Second story	Third story
Case 1	Turnbuckle (Relatively slow control)	0.0[N] → 8.0[N]	0.0[N] → 8.0[N]	0.0[N] → 8.0[N]
Case 2		-	-	0.0[N] → 8.5[N]
Case 3	Man power (Relatively fast control)	-	-	0.0[N] → 15.0[N]
Case 4		-	0.0[N] → 9.0[N]	0.0[N] → 9.0[N]

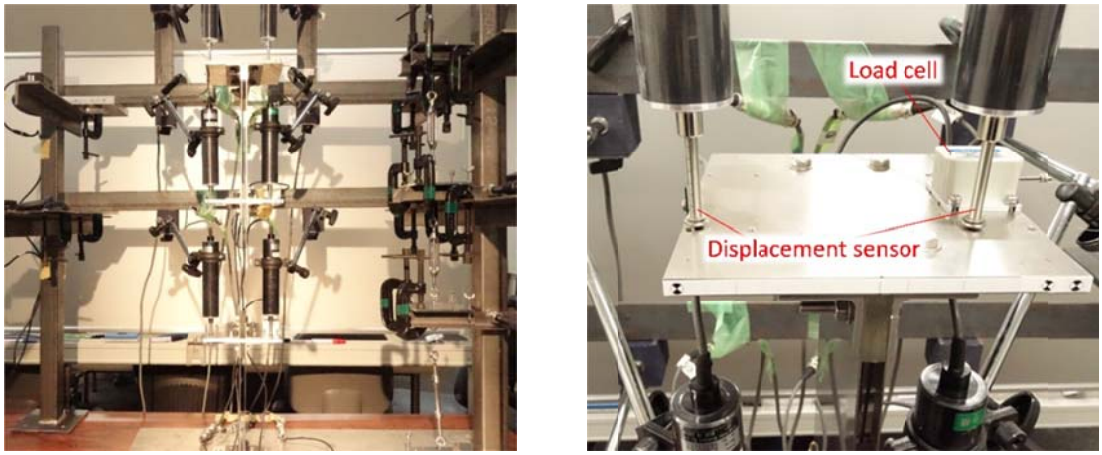

(a) (b)

Fig. 4 Photo; Static loading test (a) Setup of loading system, (b) Measurement system (top floor plate)

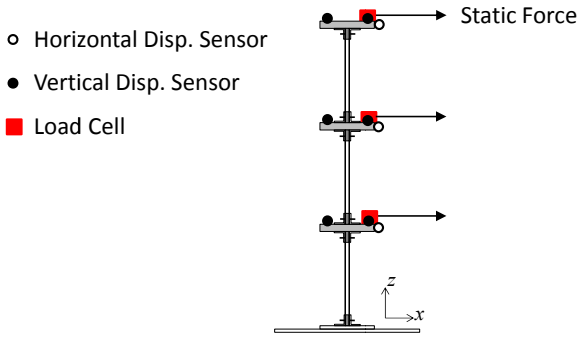

Fig. 5 Static loading and measurement position

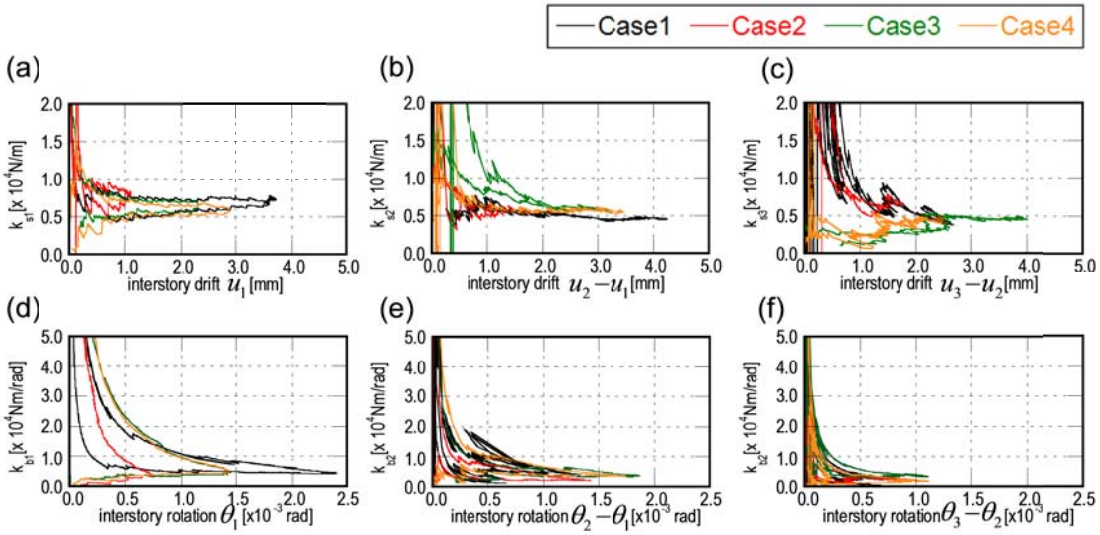

Fig. 6 Evaluation of shear and bending stiffnesses in static loading test; (a) k_{s1}vs u_1, (b) k_{s2}vs u_2-u_1, (c) k_{s3}vs u_3-u_2, (d) k_{b1}vs θ_1,(e) k_{b2}vs θ_2-θ_1,(f) k_{b3}vs θ_3-θ_2

Table 2 Estimated bounds of shear and bending stiffnesses from static loading test

	Shear stiffness [N/m]		Bending stiffness[Nm/rad]	
	Lower	Upper	Lower	Upper
first story	4.99×10^3	7.75×10^3	4.14×10^3	8.28×10^3
second story	4.19×10^3	6.53×10^3	3.36×10^3	4.91×10^3
third story	2.49×10^3	6.27×10^3	1.80×10^3	3.87×10^3

From Figs. 6(a)-(f), it can be observed that the shear and bending stiffnesses are obtained stably even though the static force distributions are different. However, the estimated shear and bending stiffnesses of the shear-bending model are dependent on amplitude. Table 2 shows the upper and lower bounds of stiffness estimated from Figs. 6(a)-(f). In this table, the lower and upper bounds of the shear stiffnesses are evaluated in the range of the interstory drift>2.0[mm] and those of the bending stiffnesses are estimated in the range of the interstory rotation angle>1.5×10^3[rad] for the second and third stories, and in the range of the interstory rotation angle>1.0×10^3[rad] for the first story.

3.3 System Identification of shear and bending stiffnesses based on vibration test

3.3.1 Shaking system for base input

A modal shaker (encapsulated type shaker, YZ-203, Asahi Manufacturing) was mainly used as the excitation source for the base input. A modal shaker was attached to the base thick plate on which the test structure is also installed. In order to excite enough vibration into the test structure, the base plate for the shaker and the test structure was placed on a linear guide with small friction. In this shaking test, the base thick plate can be regarded as the ground level for the test structure. Fig. 7. shows the photo of the setup of the test structure with the shaking system.

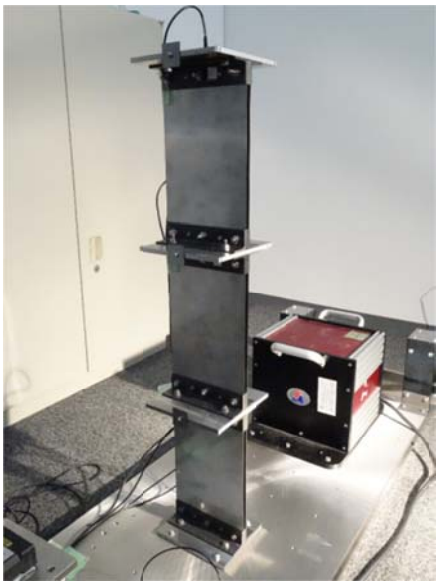

Fig. 7 Test structure with shaking system

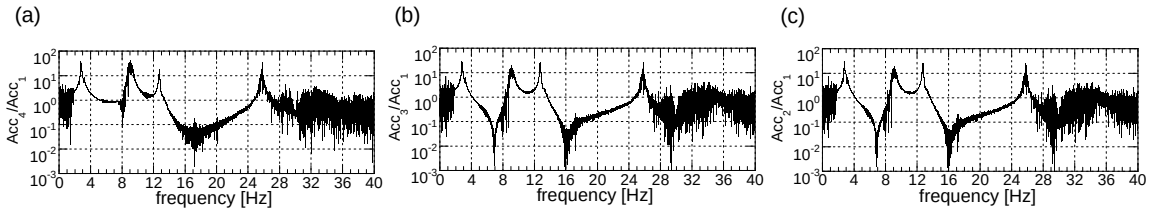

Fig. 8 Transfer function of horizontal acceleration (sweep vibration test) (a) Third story/base, (b) Second story/base, (c) First story/base

Table 3 Natural frequencies and transfer function amplitudes of test structure

mode	Natural frequency [Hz]	Transfer function amplitude		
		2F/base	3F/base	4F/base
1	2.76	16.36	29.68	38.16
2	9.06	47.32	19.33	42.63
3	12.72	18.06	25.65	17.65

3.3.2 Sweep test

So as to evaluate the modal frequencies of the test structure, the sweep test was conducted first. The target frequency band of the sweep base input was set from 2 [Hz] to 30 [Hz]. The minimum frequency control range of the shaker was limited by 2 [Hz] and a target base acceleration was controlled as 0.2 [m/s^2].

Figs. 8(a)-(c) show the transfer function of each story acceleration to the base acceleration for a record which was calculated by the ensemble average of power spectrum. Considering the control frequency band of the sweep input, the transfer functions are smoothly obtained between the target frequencies as shown in Fig. 8. The mode frequencies identified from the peak of the transfer functions and the transfer function amplitudes of the test structure are given in Table 3.

3.3.3 System identification of shear and bending stiffnesses using base input

The system identification method explained in Section 2.1 was verified by using floor accelerations under base inputs; (a) White noise, (b) El Centro NS (1940). For comparing the influence of deformation amplitude dependency caused by geometrical nonlinearity of the test structure, several cases with different input motion's amplitudes were investigated. Figs. 9(a)-(c) show the comparison of the transfer functions (Eq. (1)) of the interstory drift derived by the ARX model with that calculated by the raw data. The IDF can be described in a manner as shown in Figs. 10(a)-(c). Compared with the IDF by the raw data in Fig. 10, it can be confirmed that the IDFs using the transfer function derived by the ARX model are obtained smoothly even in the low-frequency range.

The identified shear and bending stiffnesses for various amplitudes of the base input are summarized in Figs. 11(a), (b), where the initial stiffness ratio was $\mathbf{R}=\{1\}$. In Fig. 11, the estimated bounds of those stiffnesses as the reference values (Table 1) are also shown. From Fig. 11, the variability of the identified shear stiffnesses seems to be low, while the values of the bending stiffnesses are relatively high. Similar results were observed for the base input of the white noise. Compared with the bounds obtained from the static loading tests, it is understood that the identified shear stiffnesses can be evaluated within an acceptable error. On the other hand, it

seems that the identified bending stiffnesses, especially of the lower stories, have some differences from the reference values. As explained before, since it is difficult to measure the rotation angles of the floor mass in the static loading test, the bounds of the bending stiffnesses should be regarded as merely the reference values. Fig. 12 shows the comparison of the simulated time-history acceleration of the bending-shear model, which was derived by the identified stiffnesses with damping ratio h=0.005, with that of recorded data at the top story. It can be observed from Fig. 12 that the response under base input can be simulated within an allowable accuracy by the proposed SI method.

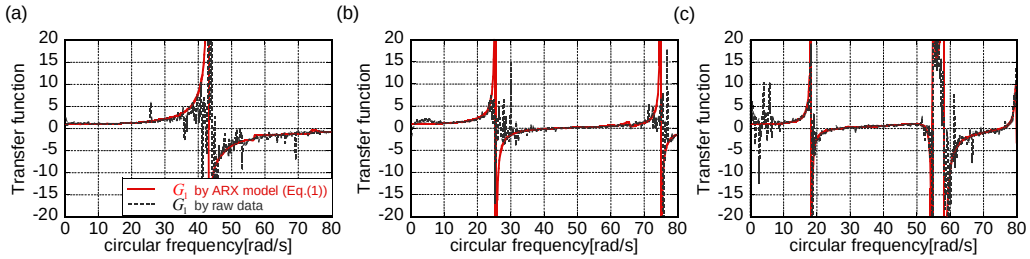

Fig. 9 Comparison of transfer functions by ARX model with that by raw data for base input (El Centro NS 10%), (a) Third story, (b) Second story, (c) First story

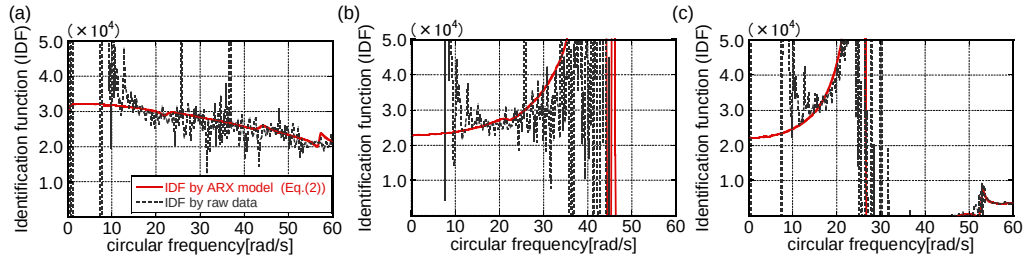

Fig. 10 Comparison of identification functions by ARX model with that by raw data for base input (El Centro NS 10%), (a) Third story, (b) Second story, (c) First story

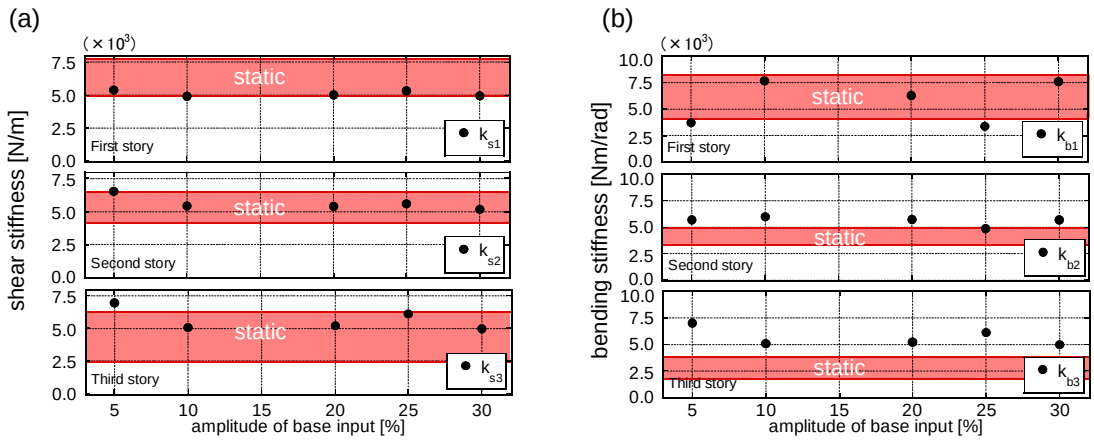

Fig. 11 Shear and bending stiffnesses identified in various amplitudes of the base input (El Centro NS), (a) Shear stiffness, (b) Bending stiffness

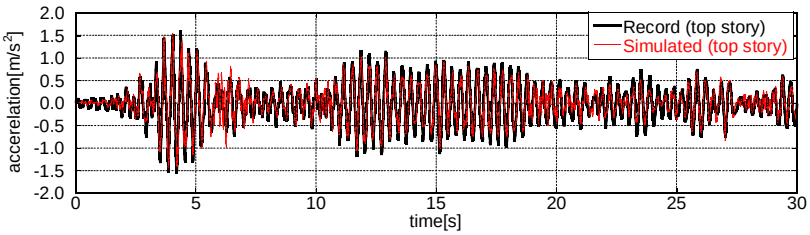

Fig. 12 Comparison of the simulated time history of the floor acceleration at the top floor with that of actual record (El Centro NS 10%, h=0.005)

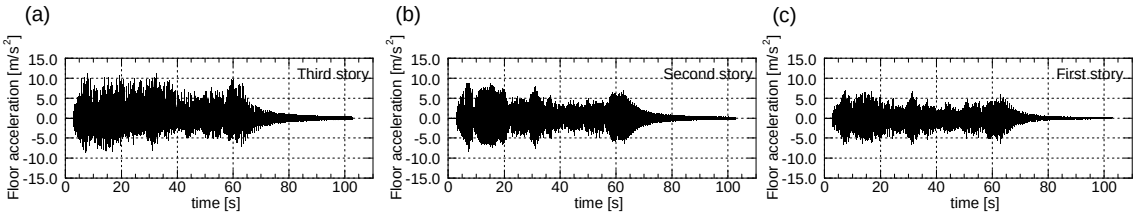

Fig. 13 Floor accelerations (man-power shaking test at the third story) (a) Third story, (b) Second story, (c) First story

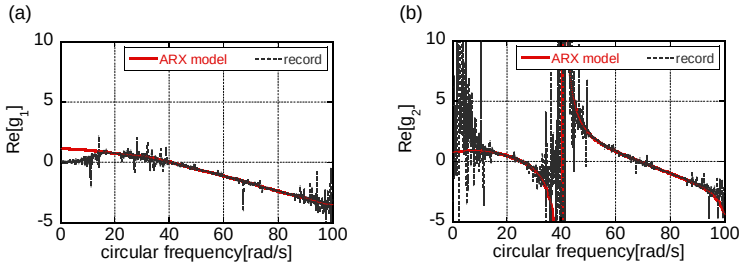

Fig. 14 Comparison of transfer functions of interstory drift ratio (a) Re[g_1], (b) Re[g_2]

3.3.4 System identification of shear and bending stiffnesses using unknown vibration source in structure

The system identification method explained in section 2.2 was also verified by using the floor accelerations under an unknown vibration source. The test structure was excited at the top floor, by man power. The accelerations on the base plate and each floor were recorded for about 60 seconds. The recorded accelerations are shown in Figs. 13(a)-(c). As mentioned in section 2.2, in applying the proposed method under an unknown vibration source, it is undesirable to cause vibration at the base. Therefore, the base plate was placed on the floor. The root mean square of the accelerations at the base was 4.69×10^{-3} [m/s^2] which was extremely smaller than 2.10 [m/s^2] at the third story.

Figs. 14(a), (b) show the comparison of the transfer function of the interstory drift ratio (Eq. (6)) derived by an ARX model with that by raw records. Since this transfer function described by the ARX model is used to identify shear and bending stiffnesses, an appropriate selection of the band pass filter is quite important in this method. The reliability of the proposed SI method will be discussed elsewhere. The identified structural properties, where the initial stiffness ratios were assumed as $\mathbf{R}=\{1\}$, are summarized in Table 4. Lower and upper frequencies of the band-path filter for the optimally identified stiffnesses were 19[rad/s] and 94[rad/s], respectively.

Table 4 Identified stiffnesses and modal frequencies of test structure

Story	Shear stiffness k_s [N/m]	Bending stiffness k_b [Nm/rad]	Stiffness ratio R	Mode	Natural circular frequency ω [rad/s]	Error ratio of ω [%]
First	5700	2565	0.45	1	17.34	-0.13
Second	4928	14178	2.88	2	56.91	0.00
Third	7494	7494	1.00	3	80.24	0.37

Table 5 Summary of the test results

SI method	Story	Shear stiffness k_s [N/m]			Bending stiffness k_b [Nm/rad]		
		Average	Standard deviation	Reference Low Upper	Average	Standard deviation	Reference Low Upper
Base Input	1	5021.3	370.7	4990 7750	6354.2	2561.2	4140 8280
	2	5580.2	421.6	4190 6530	5722.0	603.6	3360 4910
	3	5492.8	930.6	2490 6270	5492.8	930.6	1800 3870
Unknown Inner Vibration Source	1	5650.0	70.7	4990 7750	2542.5	31.8	4140 8280
	2	4995.0	94.7	4190 6530	17788.0	5106	3360 4910
	3	7324.5	239.7	2490 6270	7324.5	239.7	1800 3870

3.4 Summary of identification of shear and bending stiffnesses

The comparison of the identified shear and bending stiffnesses with the estimated bound of those stiffnesses derived by the static loading test is summarized in Table 5. In Table 5, the average and standard deviation of the stiffnesses identified by the SI method for the base input include the results for all the records of both El Centro NS and white noise inputs. On the other hand, those for an unknown vibration source were evaluated by a series of measurements.

As for the shear stiffness, by comparing the results identified by the SI method for the base input with those for an unknown vibration source, acceptable values compatible with the results by the static loading test have been obtained. On the other hand, as for the bending stiffnesses, it is concluded that the results by the SI method for an unknown vibration source are worse in view of the variability of the bending stiffness at the second story than that for the base input. This may be due to the difference of the objective function J. Since a difference between the second and third mode frequencies of the identified shear-bending model and those of the reference value is minimized in the SI method for an unknown vibration source, the variability of the natural frequencies higher than the third mode frequency caused by the change of bending stiffnesses is not necessarily reflected.

4. Conclusions

The following conclusions have been derived.

(1)The system identification theories using two consecutive floor data for a shear model and a shear-bending model were compared in detail. The theories use the base acceleration input or forced input in a building model.

(2)The system identification results by the static loading, the base acceleration input and the forced input in a building model have been compared for mutual confirmation of the reliability of these identification theories.

(3)The shear and bending stiffnesses as the reference value were derived by the static loading test. Because the difficulty exists in the loading system setup and measurement of the vertical displacements, lower and upper bounds of those stiffnesses were obtained.

(4)The shear stiffnesses of the test structure identified by the proposed SI methods were acceptable compared with those derived by the static loading test. The standard deviation of the identified story stiffness becomes larger in the upper story.

(5)The bending stiffnesses of the test structure identified by the SI method for the base input were compatible with the reference values. Those derived by the SI method for an unknown vibration source were not appropriate because of a large variability in the second story.

It should be remarked again that, because the shear-bending model is an ideal mechanical model, actual test structures cannot be modeled by this model exactly. The shear and bending stiffnesses of the shear-bending model depend on the loading distributions and the identified stiffnesses in various loading conditions do not necessarily coincide in principle. There are some SI methods developed so far. The most well-known one is the modal parameter SI which identifies the natural frequencies from the transfer functions. Furthermore some additional information may be obtained from a forced vibration test. However, it seems difficult to identify the shear and bending stiffnesses of the shear bending model directly from these natural frequencies and forced vibration data. As another method for shear models, several SI methods using repetitive algorithms have been developed (for example, Nayeri *et al*. 2008, Zhang and Johnson 2013). However these methods are not direct compared to the proposed method and cannot be applied to high-rise buildings.

Acknowledgements

The authors would like to thank Mr. Y. Minami for his help in the computation. Part of the present work is supported by the Grant-in-Aid for Scientific Research of Japan Society for the Promotion of Science (No. 24246095). This support is greatly appreciated.

References

Bendat, J.S., Palo, P.A. and Coppolini, R.N. (1992), "A general identification technique for nonlinear differential equations of motion", *Probab. Eng. Mech.*, **7**(1), 43-61.

Bendat, J.S. (1998), *Nonlinear Systems Techniques and Applications*, John Wiley and Sons, New York.

Bernal, D. and Beck, J. (2004), "Preface to the special issue on phase I of the IASC- ASCE structural health monitoring benchmark", *J. Eng. Mech.*, ASCE, **130**(1), 1-2.

Casciati, F. (2002), *Proceedings of* 3*rd World Conference on Structural Control*, John Wiley & Sons: Como.

Doebling, S.W., Farrar, C.R., Prime M.B. and Shevitz D.W. (1996). "*Damage identification and health monitoring of structural and mechanical systems from changes in their vibration characteristics: A literature review*", Los Alamos National Laboratory Report LA-13070-MS.

Fujino, Y., Nishitani, A. and Mita, A., (2010), *Proceedings of* 5*th World Conference on Structural Control and Monitoring*, *(5WCSCM)*, Tokyo, Japan.

Hart, G.C. and Yao, J.T.P. (1977), "System identification in structural dynamics", *J. Eng. Mech. Div.*, ASCE, **103**(6), 1089-1104.

Housner, G.W., Bergman, L., Caughey, T.K., Chassiakos, A.G., Claus, R.O., Masri, S.F. and Yao, J.T. (1997), "Structural control: past, present, and future", *J. Eng. Mech.*, **123**(9), 897-971.

Housner, G.W., Masri, S.F. and Chassiakos, A.G. (1994), *Proceedings of* 1*st World Conference on Structural Control*. IASC: Los Angeles, CA, USA.

Kougioumtzoglou, I.A. and Spanos, P.D. (2013), "An identification approach or linear and nonlinear time-variant structural systems via harmonic wavelets", *Mech. Sys. Signal Pr.*, **37**(1), 338-352.

Kozin, F. and Natke, H.G. (1986), "System identification techniques", *Struct. Safety*, **3**(3), 269-316.

Nayeri, R.D., Masri, S.F., Ghanem, R.G. and Nigbor, R.L. (2008), "A novel approach for the structural identification and monitoring of a full-scale 17-story building based on ambient vibration measurements", *Smart Mater. Struct*., **17**(2), 1-19.

Spanos, P.D. and Lu, R. (1995), "Nonlinear system identification in offshore structural reliability", *J. Offshore Mech. Arctic Eng*., **117**(3), 171-177.

Takewaki, I. and Nakamura, M. (2000), "Stiffness-damping simultaneous identification using limited earthquake records", *Earthq. Eng. Struct. Dyn*., **29**(8), 1219-1238.

Takewaki, I. and Nakamura, M. (2005), "Stiffness-damping Simultaneous Identification under Limited Observation", *J. Eng. Mech*., ASCE, **131**(10), 1027-1035.

Takewaki, I., Nakamura, M. and Yoshitomi, S. (2011), *System Identification for Structural Health Monitoring*, WIT Press (UK).

Johnson, E. and Smyth, A. (2006), *Proceedings of* 4*th World Conference on Structural Control and Monitoring, (4WCSCM)*. IASC: San Diego, CA, USA.

Kobori, T., Inoue, Y., Seto, K., Iemura, H. and Nishitani, A. (1998), *Proceedings of* 2*nd World Conference on Structural Control*, John Wiley & Sons: Kyoto, Japan.

Kuwabara, M., Yoshitomi, S. and Takewaki, I. (2013), "A new approach to system identification and damage detection of high-rise buildings", *Struct. Control. Hlth. Monit.*, **20**(5), 703-727.

Minami, Y., Yoshitomi, S. and Takewaki, I. (2013a), "System identification of super high-rise building using limited vibration data during the 2011 Tohoku (Japan) earthquake", *Struct. Control. Hlth. Monit.*, **20**(11), 1317-1338.

Minami, Y., Shirono, M., Fujita, K. and Takewaki, I. (2013b), "Stiffness identification of high-rise building with unknown vibration source using bending-shear model and ARX model", *J. Struct. Construct. Eng*., *AIJ*, **690**, (in Japanese).

Udwadia, F.E., Sharma, D.K. and Shah, P.C. (1978), "Uniqueness of damping and stiffness distributions in the identification of soil and structural systems", *J. Appl. Mech.*, ASME, **45**(1), 181-187.

Yoshitomi, S., Maeda, T. and Takewaki, I. (2009), "Stiffness-damping simultaneous identification of buildings including unknown inner vibration source", *J. Struct. Construct. Eng*., **74**(645), 1983-1991. (in Japanese)

Zhang, D.Y. and Johnson, E.A. (2013), "Substructure identification for shear structures I: Substructure identification method", *Struct. Control. Hlth. Monit.*, **20**(5), 804-820.